

RESEARCH ARTICLE

Traffic Modelling Framework for Electric Vehicles

Arieh Schlote^{ac*}, Emanuele Crisostomi^b, Stephen Kirkland^a and Robert Shorten^{ac}

^a*Hamilton Institute, National University of Ireland, Maynooth, Ireland*

^b*Department of Energy and Systems Engineering, University of Pisa, Italy*

^c*A. Schlote and R. Shorten are currently visiting the Technische Universität Berlin, Fachgebiet Regelungssysteme, Berlin, Germany*

(v1.0 released January 2012)

This paper reviews and improves a recently proposed model of road network dynamics. The model is also adapted and generalised to represent the patterns of battery consumption of electric vehicles traveling in the road network. Simulations from the mobility simulator SUMO are given to support and to illustrate the efficacy of the proposed approach. Applications relevant in the field of electric vehicles, like optimal routing and traffic load control, are provided to illustrate how the proposed model can be used to address typical problems arising in contemporary road network planning and electric vehicle mobility.

Keywords: road network model, Markov chain, electric vehicles, large-scale control and optimisation

1 Motivation

Urban traffic is a major contributor to pollution induced health problems in cities, and to CO_2 emissions globally. Recent reports (Qian et al. 2011) estimate that road transportation accounts for 25% of carbon emissions in the European Union. The damage to human health caused by road transportation is now recognised by both regulatory bodies, and by industry; see for example the IBM smart city initiative (Dirks et al. 2010) and Cisco's smart and connected communities initiative (Villa and Mitchell 2009). Roughly speaking, the strategy to reduce the effect of road transportation rests on three pillars: *avoid*; *shift* and *improve*¹. The first part of this strategy involves inducing change in the public to encourage alternative forms of transport; the second part of the strategy involves shifting our mobility patterns to make better use of resources; and the third involves using technology to improve existing ICE (internal combustion engine) based modes of transport.

One of the main barriers to behavioural change and to adopting new technology is the perception that the user experience will somehow suffer. For example, despite significant financial incentives, the take-up of electric vehicles in the UK is disappointing; in the first half of 2011, only 170 electric vehicles were purchased by private customers². One of the main problems with the adoption of such vehicles is the perception that the range of such vehicles is limited, and that charging times are prohibitively long. Given this background, a key issue for control engineers, is the development of tools that both facilitate more efficient use of our road networks, and enhance the user experience - especially when it comes to adopting new

*Corresponding author. Email: Arieh.Schlote@nuim.ie

¹Source: Professor D. Banister (Oxford); Public Lecture; TU-Berlin; September 29th, 2011

²Source: Professor D. Banister (Oxford); Public Lecture; TU-Berlin; September 29th, 2011

1 technology. Thus, tools that enable planners to avoid traffic delays, avoid pollution peaks,
2 and allow efficient route selection (so as to maximise driving range), are seen as key enabling
3 technologies in the area of city planning. A major component in developing such traffic manage-
4 ment strategies are accurate traffic models that can be easily used for both prediction and control.
5

6
7 Recently, one such traffic model was proposed in Crisostomi et al. (2011). This model
8 is based on the theory of Markov chains and differs considerably from conventional traffic
9 models. In the past, it was almost impossible to obtain real time data about the state of
10 traffic networks and many traffic models (Piccoli and Garavello 2006) were based on partial
11 differential equations that are necessarily very complex in order to achieve a high degree of
12 accuracy. However, recent developments and advances in vehicular technology (Hartenstein
13 and Laberteaux 2010), as for example the wide deployment of GPS communication devices
14 in cars, make it possible to collect a huge amount of data close to real time (Biem et al.
15 2010), and consequently such data can be used to develop statistical and probabilistic models
16 of road network dynamics. Such developments are the principal motivation for the work in
17 Crisostomi et al. (2011) where knowledge of the road network topology is combined with traffic
18 measurements to realistically describe the road network dynamics. An advantage of this model
19 is that it is suitable for control and is multi-variate (gathers under the same framework ap-
20 parently different phenomena such as car congestion, CO_2 emissions and other pollution agents).
21
22

23
24 The objectives and the contributions of this paper are

- 25 • to improve the mathematical consistency of the model in Crisostomi et al. (2011) and of some
26 of its properties;
- 27 • to relax the flow conservation assumptions in Crisostomi et al. (2011), and replace these with
28 more realistic ones;
- 29 • to extend the original framework to make it suitable for modelling road networks in a manner
30 that is useful for electric and hybrid electric vehicles. This objective is particularly challenging,
31 as the battery charge can both increase and decrease when electric vehicles travel in the road
32 network, thus requiring the model to be able to handle both positive and negative values;
- 33 • to present and solve a number of applications that are particularly appealing in the context
34 of electric vehicles (e.g., optimal routing, traffic load control).
35

36
37 This article is organised as follows. First we give a general overview of the Markov chain based
38 road network model, and we give a mathematical proof of its consistency. In Section 3 we derive
39 a similar model in terms of energy consumption, and we show how some negative quantities can
40 be handled within a probabilistic framework. In Section 4 we illustrate the utility of the model
41 by giving a number of applications that are relevant in the context of electric vehicles. Finally
42 in the last section we summarise the paper and outline current and future work.
43
44

45 46 2 The Markov Chain Model of Urban Traffic

47
48 In this section we briefly review the model given in Crisostomi et al. (2011). In addition we
49 further motivate the usage of this model, highlight some of its limitations, and extend the model
50 to remove some of these.
51
52

53 54 2.1 A Primer on Markov Chains

55
56 First we recall the following discussion from Crisostomi et al. (2011). A Markov chain is a
57 discrete time stochastic process, where the transition probabilities depend only on the state of
58 the chain at the previous time step and not on the past history of the process. Throughout this
59 paper we consider only time homogeneous Markov chains. We denote by \mathbb{P}_{ij} the probability
60

of going from state i to state j in one time step and if the number of states is finite, then the matrix \mathbb{P} of elements \mathbb{P}_{ij} , together with the initial distribution vector, fully describes the evolution of the Markov chain. A graph is a set of states (or nodes) that can be connected by edges (or arcs). We will only consider directed edges here. An edge from state i to state j indicates that it is possible to make a transition from state i to state j . It is possible to give a weight to each edge that corresponds to the cost of using that edge. If the aggregate cost of all outgoing edges of each node is normed to 1 then the costs can be interpreted as the probabilities of using the corresponding edges.

There is a strong link between Markov chains with finite state space and graphs. States of the chain can be associated with nodes in the graph and non-zero probabilities of transition between two states in the chain can be associated with directed edges between the corresponding nodes with the given probability as a weight. Graphs can thus be analysed using methods for Markov chains. The graph is called strongly connected if starting from any node it is possible to reach any other node by following the edges. The graph is strongly connected if and only if the transition matrix of the corresponding Markov chain is irreducible. Throughout this paper we will assume that all the Markov chain transition matrices we regard are irreducible. We can apply the Perron-Frobenius theorem, see for example Horn and Johnson (1990, Theorem 8.8.4), to ensure the existence of an invariant measure π with $\pi^T \mathbb{P} = \pi^T$. In this situation, π is entry-wise positive and its entries sum to 1; we call π the chain's stationary distribution.

An important notion in the study of irreducible Markov chains is the mean first passage time m_{ij} , which gives the expected number of steps of a random walk starting from vertex i and finishing in vertex j governed by the weights of the graph's edges (Kemeny and Snell 1960). A related concept to the mean first passage times is given by the Kemeny constant, which is the expected cost of a random trip on the graph where the destination is chosen according to the stationary distribution. For node i this value can be computed as

$$K_i = \sum_{j \neq i} m_{ij} \pi_j. \quad (1)$$

It is well known that K_i is independent of the starting node i , and thus is a global parameter for the Markov chain (Kemeny and Snell 1960). We would like to point out that the Kemeny constant is closely related to other important notions that arise in the study of Markov chains, as $K_i + 1$ is identical to the expected time to mixing, as defined in Hunter (2006).

2.2 Basic Markovian Model of Road Network Dynamics

Graphs and Markov chains can be used quite naturally to model urban traffic networks. This was first proposed in Crisostomi et al. (2011) and further developed in Crisostomi et al. (2011a) and Crisostomi et al. (2011b). The most simple version of our chain describes the transitions between road segments, i.e., the probability that a car driving along road x will drive on road y next.

The directed graph associated with the Markov chain is constructed in the following way. Each intersection in the road network is a vertex in our graph and there is an edge between two vertices if there is a road segment that connects the two corresponding intersections. An example of such a graph can be found in Figure 1, where junctions A, B, ..., G are connected by road segments. For instance, the road segment AB is the road that allows a car to go from A to B, and is different from BA which goes from B to A. We will call this our primal graph and we now describe the dual graph. In the dual graph the nodes are the edges from the primal graph, (i.e., the road segments of the traffic network), and there is an edge between two nodes if it is possible to make a direct transition between the corresponding road segments. The dual graph

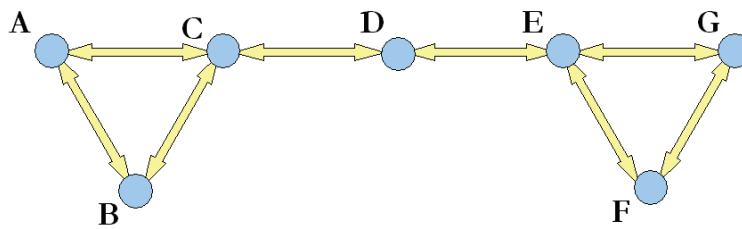


Figure 1. Example of a primal graph of an urban traffic network.

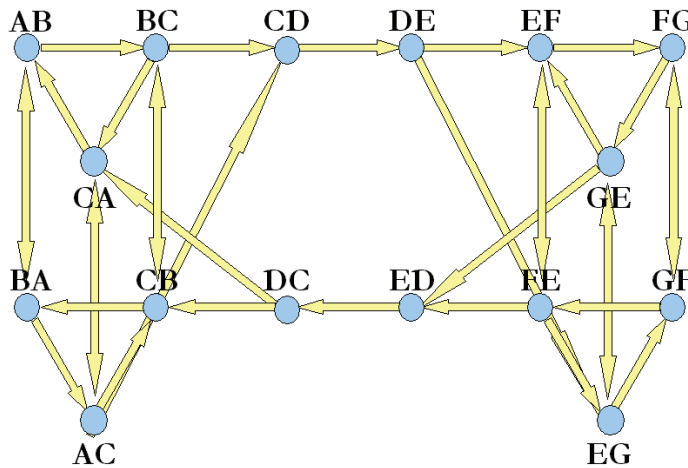


Figure 2. The dual graph corresponding to the graph shown in Figure 1.

corresponding to Figure 1 can be found in Figure 2. It can be noted that dual graphs carry more information than the corresponding primal graphs. For instance, we can see from Figure 2 that cars are not allowed to perform u-turns at junction D, while the same information can not be recovered from the primal graph in Figure 1. The weights for the edges in the dual graph are given by the turning probabilities. In the following, we are interested in the Markov chain that corresponds to the dual graph.

Comment : As there are no self-loops in this basic model, the diagonal elements of the transition matrix \mathbb{P} are all zero.

Comment : The application of a Markov chain to model road networks is well motivated. First, note that Markov chains have a large history of being used as high level approximations for complex dynamic systems. For example, the planar restricted circular three-body problem, involving a planet, a moon orbiting on a circle around the planet, and an asteroid lying on the same plane of the moon orbit, can be solved by using advanced methods from dynamic systems theory; see Koon et al. (2000, 2002). It was shown in Dellnitz et al. (2005) that similar results can be obtained by using Markov chains. Similarly, to obtain a good macroscopic description of a complicated dynamic system, the Frobenius-Perron operator can be used. The Frobenius-Perron operator describes the evolution of probability measures in time, and can be conveniently approximated using Markov chain techniques (Dellnitz and Junge 1999). Successful applications of this idea have been obtained in the modelling of complex bio molecules (Huisinga 2001, Schütte and Huisinga 2003). Finally, a comprehensive introduction to modelling complex dynamic systems as Markov chains can be found in Froyland (2001).

In our special situation the following argument can be used to motivate our study. It is clear that cars entering a road segment have to leave it again eventually. Consequently, we have asymptotic flow conservation (i.e., the long-run fraction of cars entering the road has to equal the fraction of cars leaving again). If we use $\pi \in \mathbb{R}_+^n$ to denote the long-run distribution of cars within the road network, and $p_{ij} \geq 0$ to denote the probability of going from road i to road j , then

$$\underbrace{\sum_{j=1}^n \pi_j p_{ji}}_{\text{fraction of cars entering road } i} = \underbrace{\sum_{k=1}^n \pi_i p_{ik}}_{\text{fraction of cars leaving road } i} = \pi_i \sum_{k=1}^n p_{ik} = \underbrace{\pi_i}_{\text{fraction of cars in road } i}, \quad (2)$$

where we consider the cars remaining in road i after one time step as cars leaving and re-entering road i . In matrix form Equation (2) translates into $\pi^\top P = \pi^\top$, where $P = (p_{ij})$. This is exactly the relation describing the stationary distribution that we also get from the Markov chain as described above. While this is an elementary argument, the approach is justified experimentally using SUMO¹ in Crisostomi et al. (2011). A potential problem with the approach, not discussed in Crisostomi et al. (2011), stems from the road segment conservation assumptions. In realistic situations, significant quantities of cars may park along certain routes, thereby rendering our flow assumptions invalid. As we shall see, such behaviour can be incorporated into our model, and we will relax the assumption of local flow conservation later in Section 2.4.

2.3 Multi-variate and Derivative Models

The basic Markov chain describes the probability of making a transition from one road segment to another in one step. It contains no concept of time that is required to travel or pollutants that are released. To derive the desired other models from this basic model we now modify the basic chain to describe the probability of transition per unit of time (giving a congestion chain), per unit of pollution (giving a pollution chain), and per unit of energy consumption (giving an energy consumption chain). As was first proposed in Crisostomi et al. (2011), we modify the basic chain by inserting diagonal entries to the transition matrix \mathbb{P} introduced in the previous section, and by scaling the off-diagonal entries. The diagonal entries are used in our model to account for several factors such as the length of the road, speed limits, road inclination, priority rules, traffic lights, traffic congestion and other non-trivial factors. We use some or all of the factors to compute a cost that has to be paid in order to traverse each road segment. In particular, if a cost of $w_i > 0$ is required on average to pass through state i , then the corresponding diagonal entry is chosen as

$$\tilde{w}_i = \frac{w_i - \alpha}{w_i}, \quad (3)$$

where we choose $0 < \alpha \leq \min_i w_i$. The parameter α corresponds to the cost associated with one step of the Markov chain; we call α our step size. See for instance Crisostomi et al. (2011, Appendix) to see how this was derived. We will discuss the influence of the choice of step size on the model later in this section and in Section 2.4. Let us denote with W and D the diagonal matrices $W = \text{diag}(w_1, \dots, w_n)$ and $D = \text{diag}(\tilde{w}_1, \dots, \tilde{w}_n)$ respectively. A new Markov chain

¹SUMO is an open source road traffic simulation package that was developed at the Institute of Transportation Systems at the German Aerospace Center, and is licensed under the GPL. Specifically, SUMO is used to generate data to build our Markov chain, to validate the outcomes of our modelling approach, and to illustrate other merits of the Markovian approach.

transition matrix \mathbb{Q} is then obtained by

$$\mathbb{Q} = (\mathbf{I} - D)\mathbb{P} + D \quad (4)$$

where \mathbf{I} is the identity matrix of appropriate dimensions. It can be easily noted that \mathbb{Q} is again row-stochastic, and the expected number of steps before leaving the state i is proportional to w_i and the ratios between the off-diagonal terms in each row are the same as in the initial transition matrix \mathbb{P} . The following lemma presents an alternative way of computing the left Perron eigenvector of \mathbb{Q} . It is a rigorous presentation of an observation from Crisostomi et al. (2011).

Lemma 2.1: *Let \mathbb{P} be irreducible and let π^\top be the left Perron eigenvector of \mathbb{P} , then $(W\pi)^\top$ is the left Perron eigenvector of \mathbb{Q} .*

Proof \mathbb{Q} has a left Perron eigenvector as it is non-negative and has the same sign structure as \mathbb{P} off the diagonal and is thus irreducible. The claim is then proved by noting that $D = \mathbf{I} - \alpha W^{-1}$, $\mathbb{Q} = \mathbf{I} + \alpha W^{-1}(\mathbb{P} - \mathbf{I})$ and the following.

$$\begin{aligned} (W\pi)^\top \mathbb{Q} &= (W\pi)^\top (\mathbf{I} + \alpha W^{-1}(\mathbb{P} - \mathbf{I})) \\ &= \pi^\top W^\top + \alpha \pi^\top W^\top W^{-1} \mathbb{P} - \alpha \pi^\top W^\top W^{-1} \\ &= (W\pi)^\top. \end{aligned}$$

□

The next Lemma shows that all generalised eigenvectors of \mathbb{Q} are independent of the step size α , but the corresponding eigenvalues are not. We give α as an argument whenever a quantity depends on α .

Lemma 2.2: *Let α_1, α_2 be positive step sizes. Then any right (or left) (generalised) eigenvector x of $\mathbb{Q}(\alpha_1)$ is also a right (or left) (generalised) eigenvector of $\mathbb{Q}(\alpha_2)$, and vice versa. Further, for a common right (or left) (generalised) eigenvector the corresponding eigenvalues, $\lambda(\mathbb{Q}(\alpha_1))$ and $\lambda(\mathbb{Q}(\alpha_2))$, are related as*

$$\frac{\lambda(\mathbb{Q}(\alpha_1)) - 1}{\alpha_1} = \frac{\lambda(\mathbb{Q}(\alpha_2)) - 1}{\alpha_2}. \quad (5)$$

Proof The proof is based on the special form of $\mathbb{Q}(\alpha)$, namely $\mathbb{Q}(\alpha) = \alpha W^{-1}(\mathbb{P} - I) + I$. Each of $\mathbb{Q}(\alpha)$, $\mathbb{Q}(\alpha) - I$ and $\frac{1}{\alpha}(\mathbb{Q}(\alpha) - I)$ has a common (right or left) Jordan basis. As $\frac{1}{\alpha}(\mathbb{Q}(\alpha) - I) = W^{-1}(\mathbb{P} - I)$ is independent of α , we see that any right or left Jordan basis for $\mathbb{Q}(\alpha_1)$ is also a right or left Jordan basis for $\mathbb{Q}(\alpha_2)$. This proves the claim on the eigenvectors. Further, note that if x is a right eigenvector for $\mathbb{Q}(\alpha_1)$ with eigenvalue $\lambda(\mathbb{Q}(\alpha_1))$, then x is also a right eigenvector for $\frac{1}{\alpha_1}(\mathbb{Q}(\alpha_1) - I)$ with eigenvalue $\frac{\lambda(\mathbb{Q}(\alpha_1)) - 1}{\alpha_1}$; it now follows that x is also a right eigenvector for $\frac{1}{\alpha_2}(\mathbb{Q}(\alpha_2) - I)$ with eigenvalue $\frac{\lambda(\mathbb{Q}(\alpha_2)) - 1}{\alpha_2}$, and hence that $\frac{\lambda(\mathbb{Q}(\alpha_1)) - 1}{\alpha_1} = \frac{\lambda(\mathbb{Q}(\alpha_2)) - 1}{\alpha_2}$. □

As further explained in the remainder of this section, W represents a diagonal matrix of appropriate weights that accounts for the average time, or the average quantity of emissions that is spent or released along each road segment. We use W to transform the basic Markov chain described by the transition matrix \mathbb{P} to a new chain with transition matrix \mathbb{Q} ; doing so we now describe two known application areas for the Markov chain model before extending the model to a new area in the next section.

The Congestion Chain: The congestion chain describes vehicular traffic in the urban network and is governed by a unit of time (i.e., vehicles change a state after a certain amount

Table 1. Interpretation of some Markov chain quantities of interest in the congestion application

Quantity / Markov chain	Congestion chain
Perron Eigenvector (dual)	Vehicular density in the network
Mean First Passage Times	Average travel times for a pair of origin/destination
Kemeny constant	Average travel time for a random trip
Perron Eigenvector (primal)	Congested junctions in the network
Second Eigenvector (dual)	Associates nodes to traffic sub-communities

Table 2. Interpretation of some Markov chain quantities of interest in the pollution application

Quantity / Markov chain	Pollution chain
Perron Eigenvector (dual)	Pollutant density in the network
Mean First Passage Times	Average pollution for a pair origin/destination
Kemeny constant	Average pollution for a random trip
Perron Eigenvector (primal)	Polluted junctions in the network
Second Eigenvector (dual)	Associates nodes to pollutant sub-communities

of time). Thus, the weight matrix W accounts for the average time required to traverse a road segment. This congestion chain was widely discussed and validated in Crisostomi et al. (2011), where it was shown that results similar to those obtained by using conventional mobility simulators (e.g., SUMO (Krajzewicz et al. 2006)) can be found in a much more efficient manner with the Markov chain approach. In addition, the chain gives much faster predictions, and yields other predictions not readily obtained from conventional simulators, such as expected travel times, network efficiency, etc.

The Pollution Chain: The main difference between the previous congestion chain and the pollution chain is that now the state is changed as soon as a unit of pollutant is emitted. Therefore the diagonal matrix of weights W accounts for the different quantities of pollutants that are emitted along each road segment, as described with more details in Crisostomi et al. (2011b). Our chain is constructed from an emission model that relates fuel consumption or pollutant emission to the vehicle average speed (plus other determinant factors such as the type of vehicle).

As can be seen from the previous two examples, the same basic Markov chain containing only turning probabilities can be used as a starting point for different applications, where the diagonal matrix W is used to differentiate final results. Perhaps the most attractive feature of the proposed paradigm is that typical Markov chain quantities of interest have a straightforward interpretation in the applications. This is summarised in Tables 1 and 2.

2.4 Alternative Flow Conservation Assumptions

As we have already mentioned, a basic problem in the model (Crisostomi et al. 2011) is that the flow conservation assumptions made to derive the model are not realistic. While it is relatively straightforward to overcome the limitations imposed by these assumptions, it is an oversight in the work described in Crisostomi et al. (2011), that these limitations are neither discussed nor resolved there. We would like to point out however that this assumption is widely used in traffic modelling. This is especially true for flow based methods and these assumptions underlie many fluid models (Hartenstein and Laberteaux 2010). It should be noted that this assumption is realistic in highway networks (Baskar et al. 2011) or single junctions (Piccoli and Garavello 2006, Moya and Poznyak 2009), but can not be generalised to an urban network level. We now rectify this matter by describing a basic modification to our Markov chain that resolves these issues.

Clearly, the assumption of local flow conservation is not correct in real traffic networks. Other conservation assumptions are more reasonable. For example, it is reasonable to consider the total amount of cars in a city as being constant, or to assume that as one car enters a parking state, another car ("somewhere") starts a journey. Consequently, there are at least two

1 methods of overcoming the limitations of the model in Crisostomi et al. (2011). We now present
 2 these two modifications. Afterwards, somewhat surprisingly, we show that both approaches give
 3 equivalent results in terms of the stationary distribution.
 4

5 Motivated by the work underpinning the PageRank (Langville and Meyer 2006) algorithm,
 6 for the first approach we require that when a car reaches its destination, somewhere else a
 7 new car starts its journey. This gives our model two additional degrees of freedom. For each
 8 road segment we have a probability that a car will leave or enter the road network at this
 9 segment. This allows to model a large number of scenarios. We will refer to this approach as
 10 the teleportation approach.
 11

12 The second approach is inspired by the theory of semi-open Jackson networks (Chen and Yao
 13 2001). To keep the total number of users in such a network of queues at a constant level, an
 14 extra state is added to the model. This extra state represents users that have departed to the
 15 outside world. While the number of customers in the extended network is constant, the number
 16 of customers which is in the original network is variable but bounded. We do the same thing
 17 for our road network. We add an extra state that is connected to all other road segments, so a
 18 car can finish its journey in a “parked” state. With the probabilities of going to the extra state
 19 from each road segment and of going to each road segment from the extra state we have here
 20 the same parameters as in the teleportation approach, but at the cost of having an extra state
 21 we gain the possibility of influencing the time cars spend outside the network. Note that we can
 22 also include cars physically leaving the regarded road network (for example by leaving the city)
 23 into this framework.
 24

25 We now present the technical details of how transition matrices for our Markov chain
 26 corresponding to the two approaches can be obtained. We will then show that the respective
 27 stationary distributions are equivalent and independent of the weight of the self-loop of the
 28 extra state.
 29

30 Let $Q = [q_{ij}] \in \mathbb{R}^{n \times n}$ be the matrix counting transitions between streets, $p \in \mathbb{R}^n$ the vector
 31 that counts the number of times each road segment is the origin of a route, and $q \in \mathbb{R}^n$ the
 32 vector that counts the number of times each road segment is the destination of a route. We
 33 will throughout this section assume that neither p nor q is the zero vector and that Q is an
 34 irreducible matrix. Let $\tilde{p} = \frac{p}{\|p\|_1}$.
 35

36 For the teleportation approach let
 37

$$38 \quad \tilde{U} = Q + q\tilde{p}^T. \quad (6)$$

39 We now make this matrix row stochastic by scaling it in the following way
 40

$$41 \quad U = F\tilde{U}, \quad (7)$$

42 where $F = \text{diag}(f_1, \dots, f_n)$ with
 43

$$44 \quad f_i = \left(\sum_{j=1}^n q_{ij} + q_i \left(\sum_{j=1}^n \tilde{p}_j \right) \right)^{-1} = \left(\sum_{j=1}^n q_{ij} + q_i \right)^{-1}. \quad (8)$$

45 U is now row stochastic and describes the transitions in the chain without the extra state.
 46
 47
 48
 49
 50
 51
 52
 53
 54
 55
 56
 57
 58
 59
 60

Now we describe the transition matrix for the extra state Markov chain. Let c be a positive number that we may later use to influence the dwell time in the extra state and let

$$\tilde{\mathbb{V}} = \begin{bmatrix} Q & q \\ p^\top & c \end{bmatrix}. \tag{9}$$

We now make this row stochastic by

$$\mathbb{V} = G\tilde{\mathbb{V}}, \tag{10}$$

where $G = \text{diag}(g_1, \dots, g_{n+1})$ with

$$g_i = \left(\sum_{j=1}^n q_{ij} + q_i \right)^{-1} \tag{11}$$

for $i = 1, \dots, n$ and $g_{n+1} = (c + \sum_{j=1}^n p_j)^{-1}$ and thus

$$G = \begin{bmatrix} F & 0 \\ 0 & (\sum_{j=1}^n p_j)^{-1} \end{bmatrix}. \tag{12}$$

\mathbb{V} is now row stochastic and describes the transitions in our chain with the extra node. The following lemma explains in which sense the two approaches yield equivalent stationary distributions; it is a consequence of a well known result presented in Meyer (1989).

Lemma 2.3: *Let x^T be the stationary distribution of \mathbb{V} , with $x = \begin{pmatrix} \tilde{x} \\ x_{n+1} \end{pmatrix}$. Then $\frac{1}{1-x_{n+1}}\tilde{x}^T$ is the stationary distribution of \mathbb{U} .*

Proof We have $x^\top = x^\top \mathbb{V}$ and from this we obtain the two equations

$$x_{n+1} = \tilde{x}^\top Fq + \frac{cx_{n+1}}{c + \sum_{j=1}^n p_j} \tag{13}$$

and

$$\tilde{x}^\top = \tilde{x}^\top FQ + x_{n+1} \frac{p^\top}{c + \sum_{j=1}^n p_j}. \tag{14}$$

Solving Equation (13) for x_{n+1} and substituting in Equation (14) yields

$$\tilde{x}^\top = \tilde{x}^\top FQ + \left(\frac{\tilde{x}^\top Fq}{1 - \frac{c}{c + \sum_{j=1}^n p_j}} \right) \frac{p^\top}{c + \sum_{j=1}^n p_j} = \tilde{x}^\top (FQ + Fq\tilde{p}^\top) = \tilde{x}^\top \mathbb{U}.$$

Normalising with respect to the one-norm we obtain that $\frac{1}{1-x_{n+1}}\tilde{x}^\top$ is the left Perron vector of \mathbb{U} .

□

Comment : The Markov chain with transition matrix \mathbb{U} is useful for modelling mobility patterns in the network. In particular, the vectors p and q can be used to model time-dependent directionality. For example, in the morning more cars leave the network in the city center whereas in the evening the opposite is true.

Comment : The Markov chain with transition matrix \mathbb{V} is useful when in addition one wishes to regulate the number of cars in the parked state. Encouraging people to use their cars instead of other modes of transportation could be sensible in the following two situations for example. Either when the public transportation network is operating above its capacity, or - if a significant part of the vehicles are electric vehicles or plug-in hybrid electric vehicles - the load on the public power grid is too high.

2.5 Consistency of Approach

We have thus far analysed how eigenvalues and eigenvectors behave as we change the chain's step size $\alpha > 0$. A natural question to ask is whether the Markov chain itself is well behaved when the step size approaches 0 as a limit. By this we mean that one step at a given step size or two steps at half the step size and so on should yield the same result. For completeness we now end this section of the paper by giving a result that answers this question. To this end let $A = W^{-1}(\mathbb{P} - (I))$, then we obtain $\mathbb{Q}(\alpha) = \mathbf{I} + \alpha A$. In the following theorem we denote by $\exp(\cdot)$ the matrix exponential function.

Theorem 2.4: *The limit $\lim_{k \rightarrow \infty} \mathbb{Q}(\frac{\alpha}{k})^k$, where $k \in \mathbb{N}$, exists and is equal to $\exp(\alpha A)$.*

Proof We know from Lemma 2.2 that the generalised eigenvectors of $\mathbb{Q}(\alpha)$ are independent of $\alpha > 0$. Thus all matrices $\mathbb{Q}(\alpha)$ and A are simultaneously similar to their respective Jordan canonical forms. Let $J = S^{-1}AS$ be the Jordan form of A . Then

$$\left(\mathbb{Q}\left(\frac{\alpha}{k}\right)\right)^k = \left(\mathbf{I} + \frac{\alpha}{k}A\right)^k = \left(\mathbf{I} + \frac{\alpha}{k}SJS^{-1}\right)^k = S\left(\mathbf{I} + \frac{\alpha}{k}J\right)^k S^{-1} \quad (15)$$

By regarding each individual Jordan block, it can be seen that

$$\lim_{k \rightarrow \infty} \left(\mathbf{I} + \frac{\alpha}{k}J\right)^k = \exp(\alpha J). \quad (16)$$

And hence $\lim_{k \rightarrow \infty} \left(\mathbb{Q}\left(\frac{\alpha}{k}\right)\right)^k = S \exp(\alpha J) S^{-1} = \exp(\alpha A)$. \square

Comment : This result is important to show consistency of our approach. We now also have a way of deriving a continuous time Markov process. Further its density matrix is αA , which is readily computable from the turning probabilities and the weight matrix W .

3 Electric Vehicles

In this section we show how energy consumption in electric vehicles can be integrated into the framework described above. By energy consumption we mean the charge removed from the battery when traversing a road segment. Roughly speaking, following a model presented in MacKay (2008), in Section 3.1 we calculate this charge using basic formulae from physics and assuming constant losses within the car. These internal losses are to the most part due to the transmission, the motor, and the battery.

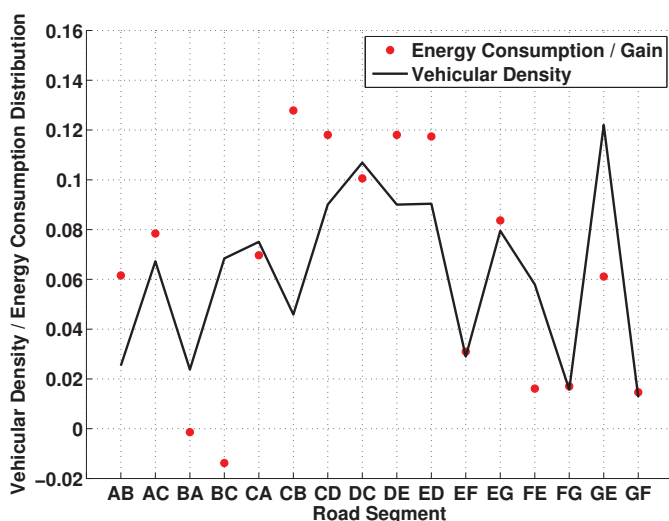


Figure 3. Comparison of distribution of cars (line) and the average amount of energy used or gained on each road segment (dots). The energy consumption distribution is positive on road segments where on average energy is expended and negative where energy is gained.

Electric vehicles differ from combustion driven vehicles in a number of aspects. Energy is scarce in such vehicles, and significant dissipation is related to road topology, to on-board systems (air conditioning, heating), and to other factors considered not important in ICE based vehicles. A very important feature is regenerative braking. Electric vehicles can recover some kinetic energy back to battery charge during the braking process. This gives rise to the possibility of negative costs on some road segments (energy transferred from the road to the vehicle). However, as we will see in Section 3.2, we can still use the base Markov chain, and from this deduce the expected energy consumption along all roads. In this sense a stationary set of expected energy consumptions may still be calculated (even though, counter-intuitively, some of these have negative values). In particular, Lemma 2.1 still holds in the sense that $(Wx)^T$ is still an eigenvector of Q corresponding to the eigenvalue 1.

Consider again the network depicted in Figure 1. Simulating with SUMO and using the Markov chain model, where we use the expected energy consumption as weights, we obtain Figure 3. It depicts the vehicular density as measured from SUMO (solid line) and $(Wx)^T$ (red dots), the extended notion of the stationary distribution of battery charge consumption/gain, as described above. For the simulation we lift junction B to be at the top of a small hill. Note that energy consumption increases drastically on the upward slopes.

3.1 Electric Consumption Model

We now present an elementary model of energy consumption in electric vehicles. Before proceeding, it is important to note that the details of this model are not important; any more accurate model can be embedded in our Markovian framework.

A first approach to modelling the energy consumption is to calculate an expected power needed for a vehicle per unit time, and to multiply this by the expected travel time. The average power (constant speed model) can be obtained as a function of: (1) average speed of the car and (2) the slope of the road. An improvement on such a basic model is to also consider the vehicle acceleration, as suggested in MacKay (2008). This is the approach followed here.

We will assume a driving pattern, where cars are stationary at the beginning of each road

segment and accelerate at a constant rate a_1 until they reach the cruising speed, v_{cruise} , and then decelerate at a constant rate a_2 to reach the end of the road segment with zero velocity. The energy can be calculated as the sum of the energies in the acceleration phase, the cruising phase and the deceleration phase.

The following forces affect the vehicle:

- $F_{acc} = ma$ is the force needed to accelerate/decelerate the car
- $F_{rol} = \mu_{rol}mg$ is the force needed to overcome the rolling resistance
- $F_{ad} = \frac{1}{2}\rho AC_d v^2$ is the aerodynamic drag force
- $F_{slope} = mg \sin(\phi)$ is the hill climbing force,

where a is the vehicle's acceleration, A is its frontal area, m its mass and v its speed, μ_{rol} , ρ , C_d and g are constants and ϕ is the inclination of the road segment. For our calculations we assume a car weight of 1235 kg, gravitational acceleration of $g = 9.81 \text{ m/s}^2$. Further reasonable parameter choices for a medium size electric vehicle are: $\rho = 1.2 \text{ kg m}^3$, $\mu_{rol} = 0.01$, $C_d = 0.35$, $A = 1.6 \text{ m}^2$ (MacKay 2008).

We will assume the slope along a road segment is constant. In general (given an accurate velocity profile) we can calculate the energy expended as the integral of the force over the path. As discussed above we split this in three parts.

$$W = \underbrace{\int_0^{x_1} (F_{acc} + F_{rol} + F_{ad} + F_{slope}) dx}_{W_1} + \underbrace{\int_{x_1}^{x_2} (F_{rol} + F_{ad} + F_{slope}) dx}_{W_2} \quad (17)$$

$$+ \underbrace{\int_{x_2}^{x_3} (F_{acc} + F_{rol} + F_{ad} + F_{slope}) dx}_{W_3}, \quad (18)$$

where x_1 is the distance after which the cruising speed is reached and x_2 is the distance after which the deceleration process is started and x_3 marks the end of the road segment. If we regard speed and distance as functions of time t and denote them $v(t)$ and $s(t)$ respectively, then speed, time, distance are related by

$$v(t) = v(0) + at \quad (19)$$

$$s(t) = s(0) + v(0)t + \frac{1}{2}at^2, \quad (20)$$

where $a \in \mathbb{R}$ is the constant acceleration rate.

We also assume a constant acceleration and deceleration rate of $a_1 = -a_2 = 3\frac{\text{m}}{\text{s}^2}$. If the length of the road, x_3 , is large enough, we obtain

$$x_1 = \frac{1}{2}a_1 t_{acc} = \frac{1}{2}a_1 \left(\frac{v_{cruise}}{a_1} \right)^2 = \frac{1}{2} \frac{v_{cruise}^2}{a_1} \quad (21)$$

$$x_2 = x_3 + \frac{1}{2} \frac{v_{cruise}^2}{a_2}, \quad (22)$$

where t_{acc} is the time it takes to accelerate the vehicle to cruising speed at rate a_1 and v_{cruise} is the cruising speed. Thus

$$\begin{aligned}
 W_1 &= \int_0^{x_1} \left(ma_1 + \mu_{rol}mg + \frac{1}{2}\rho AC_d v^2 + mg \sin(\phi) \right) dx \\
 &= \frac{1}{2}mv_{cruise}^2 + \frac{1}{2}\frac{v_{cruise}^2}{a_1}mg(\mu_{rol} + \sin(\phi)) + \frac{1}{4}\rho AC_d \frac{v_{cruise}^4}{a_1}.
 \end{aligned} \tag{23}$$

For the second integral we obtain

$$\begin{aligned}
 W_2 &= \int_{x_1}^{x_2} \left(\mu_{rol}mg + \frac{1}{2}\rho AC_d v^2 + mg \sin(\phi) \right) dx \\
 &= \left(x_3 + \frac{1}{2}\frac{v_{cruise}^2}{a_2} - \frac{1}{2}\frac{v_{cruise}^2}{a_1} \right) \left(mg(\mu_{rol} + \sin(\phi)) + \frac{1}{2}\rho AC_d v_{cruise}^2 \right)
 \end{aligned} \tag{24}$$

and for the third integral

$$\begin{aligned}
 W_3 &= \int_{x_2}^{x_3} \left(ma_2 + \mu_{rol}mg + \frac{1}{2}\rho AC_d v^2 + mg \sin(\phi) \right) dx \\
 &= (ma_2 + mg(\mu_{rol} + \sin(\phi))) \left(-\frac{1}{2}\frac{v_{cruise}^2}{a_2} \right) - \frac{1}{4}\rho AC_d \frac{v_{cruise}^4}{a_2}.
 \end{aligned} \tag{25}$$

We further assume that the losses along the drive train are a constant 15% and during deceleration 50% of the energy can be saved by regenerative braking. An additional and highly important factor in the consumption of battery load is on-board equipment such as heating, light, air-conditioner, radio and many others that draw power at constant rate over time. Their demand is much harder to model as it depends on the individual driver. However, their aggregate effect can not be neglected as will be exemplified in Section 4.2.

We now have a way to approximate energy requirements for traversing given road segments. Because of the regenerative braking it is possible that the energy requirement takes a negative value, meaning that a vehicle gains energy by traversing that road segment. Next we deal with the question, as to how our framework extends to the case where we have negative weights on some road segments.

3.2 Networks with Negative and Positive Weights

In Section 2.3 a diagonal matrix D was used to transform the basic Markov chain \mathbb{P} into a new Markov chain \mathbb{Q} , whose step unit can be different from the unit of time (e.g., can be a unit of energy). This was done in Equation (4), which we recall here for convenience:

$$\mathbb{Q} = (\mathbf{I} - D)\mathbb{P} + D. \tag{26}$$

In the case of electric vehicles, the mechanism of regenerative braking can cause non-positive entries in the diagonal matrix W . In order to apply our previously developed theory, we will make the assumption that the energy required to travel along a road i can not be exactly zero, otherwise the corresponding weight w_i would be equal to 0 and in turn this would disallow using Equation (3) to calculate the diagonal matrix D . Negative entries on the diagonal of W imply that \mathbb{Q} is not necessarily a transition matrix of a Markov chain, it might not be stochastic anymore (since it might not be non-negative and row sums can be different from 1),

so standard methods to analyse Markov chains do not apply. We note that Lemma 2.1 still holds in the sense that even if we allow negative entries in the diagonal matrix W then for all step sizes $\alpha > 0$, such that D is non-singular, the vector $(Wx)^\top$ is still a left eigenvector of the matrix \mathbb{Q} as defined in Equation (26) to the eigenvalue 1. However the matrix \mathbb{Q} and its eigenvectors do not seem to have a straightforward interpretation as in the case of all positive weights.

To be able to use the theory presented in this paper, we define an intermediate Markov chain whose step unit is a unit of energy exchanged between the vehicle and the road network, regardless of whether such a unit of energy was spent or gained (thanks to regenerative braking). To do this we define \widetilde{W} to be the diagonal matrix that contains the absolute values of all weights, $\widetilde{W} = \text{diag}(|w_1|, \dots, |w_n|)$. Accordingly we define $\widetilde{D} = \mathbf{I} - \alpha \widetilde{W}^{-1}$, where now $0 < \alpha \leq \min_i |w_i|$. We then obtain the transition matrix of the intermediate chain from

$$\widetilde{\mathbb{Q}} = (\mathbf{I} - \widetilde{D})\mathbb{P} + \widetilde{D}. \quad (27)$$

We are interested in storing memory of the sign of energy exchange (i.e., to compute the actual energy required to travel a given route). We assume that transitions between streets occur at the end of the energy step, and that the gain or loss of energy while driving along road segment i is independent of the choice of the next road segment j . With these assumptions in place, we introduce the notation σ_i to indicate the sign of the change in energy transferred from the vehicle to the network. That is, $\sigma_i = 1$ if the vehicle loses energy driving along road i , and $\sigma_i = -1$ if the vehicle gains energy driving along road i .

As the quantity of interest is energy instead of time, we use the term mean first passage energy (MFPE) instead of mean first passage time in this context. We use the intermediate Markov chain to calculate a generalised version of MFPE (generalised to include possible negative values), following and extending the approach of Grinstead and Snell (2003): For $j \neq i$, to calculate m_{ij} , the MFPE from i to j , we observe that in going from i to j we make a direct transition with probability $\widetilde{\mathbb{Q}}_{ij}$ and spend σ_i units of energy. With probability $\widetilde{\mathbb{Q}}_{ik}$ we make a transition to $k \neq j$ where we again spend σ_i units of energy to get to k , in addition the expected energy required to get from k to j is equal to m_{kj} . Thus for $j \neq i$

$$\begin{aligned} m_{ij} &= \widetilde{\mathbb{Q}}_{ij}\sigma_i + \sum_{k \neq j} \widetilde{\mathbb{Q}}_{ik}(m_{kj} + \sigma_i) \\ &= \sum_{k \neq j} \widetilde{\mathbb{Q}}_{ik}m_{kj} + \sum_{k=1}^n \widetilde{\mathbb{Q}}_{ik}\sigma_i \\ &= \sum_{k \neq j} \widetilde{\mathbb{Q}}_{ik}m_{kj} + \sigma_i. \end{aligned} \quad (28)$$

For any fixed $j = 1 \dots, n$ we can write this in vector form

$$m_{(j)} = \widetilde{\mathbb{Q}}_{(j)}m_{(j)} + \sigma_{(j)}, \quad (29)$$

where $m_{(j)} = (m_{1j}, m_{2j}, \dots, m_{(j-1)j}, m_{(j+1)j}, \dots, m_{nj})^\top$ and equivalently $\sigma_{(j)}$ is the vector of all σ_i for $i \neq j$ and $\widetilde{\mathbb{Q}}_{(j)}$ is the matrix $\widetilde{\mathbb{Q}}$ where we have eliminated the j -th row and column. Now we can calculate m_{ij} for all $i \neq j$ using the formula

$$m_{(j)} = (\mathbf{I} - \widetilde{\mathbb{Q}}_{(j)})^{-1}\sigma_{(j)}, \quad (30)$$

where we use the fact that $(\mathbf{I} - \tilde{\mathbf{Q}})$ is a singular, irreducible M-matrix and according to Berman and Plemmons (1994, Theorem 4.16) each of its proper principal submatrices is invertible.

Comment : Note that Equation (30) is identical to a standard formula for calculating mean first passage times in the case of positive weights only. As we have shown it still works if we have negative weights in the chain.

As in the case of positive weights we are interested in the Kemeny constant as a global efficiency measure, but if we introduce negative weights in our graph, Equation (1) is no longer independent of the starting node i . However we can generalise the notion of the Kemeny constant in the following way. Let π be the Perron eigenvector of $\tilde{\mathbf{Q}}$ and let

$$K = \sum_{i=1, \dots, n} \pi_i K_i = \sum_{i=1, \dots, n} \pi_i \sum_{j \neq i} \pi_j m_{ij}. \quad (31)$$

Then K coincides with the Kemeny constant as defined in Equation (1) in the case where all weights are positive.

In the spirit of Lemma 2.2, the following lemma shows that generalised mean first passage energies and the generalised Kemeny constant scale linearly with the step size.

Lemma 3.1: For given step sizes $\alpha_1, \alpha_2 > 0$ and for all $i, j = 1, \dots, n$ we get $\alpha_1 m_{ij}(\alpha_1) = \alpha_2 m_{ij}(\alpha_2)$ and $\alpha_1 K(\alpha_1) = \alpha_2 K(\alpha_2)$.

Proof From Equation (30) we have

$$\begin{aligned} m_{(j)}(\alpha_1) &= (\mathbf{I} - \tilde{\mathbf{Q}}_{(j)}(\alpha_1))^{-1} \sigma_{(j)} = (-\alpha_1 \tilde{\mathbf{W}}^{-1}(\mathbb{P} - \mathbf{I}))_{(j)}^{-1} \sigma_{(j)} \\ &= \frac{\alpha_2}{\alpha_1} (-\alpha_2 \tilde{\mathbf{W}}^{-1}(\mathbb{P} - \mathbf{I}))_{(j)}^{-1} \sigma_{(j)} = \frac{\alpha_2}{\alpha_1} m_{(j)}(\alpha_2), \end{aligned} \quad (32)$$

where again by $(-\alpha_1 \tilde{\mathbf{W}}^{-1}(\mathbb{P} - \mathbf{I}))_{(j)}$ we denote the matrix $(-\alpha_1 \tilde{\mathbf{W}}^{-1}(\mathbb{P} - \mathbf{I}))$ where we have eliminated the j -th row and column. The claim about the generalised Kemeny constant now follows directly from its definition, Equation (31). \square

4 Applications

We now give a number of applications to illustrate the utility of our model. The first application illustrates the effect of relaxing the flow conservation assumptions in Crisostomi et al. (2011). The second application concerns using the model for routing. This idea is already explored in the context of conventional vehicles in Crisostomi et al. (2011a) and we now suggest how this basic idea can be used for routing of electric vehicles. In the third example we investigate how the Markov chain can be controlled both in an idealised context (using Lemma 2.1), and in a practical context using decentralised control.

4.1 Realistic Traffic Model: Relaxed Flow Conservation Assumptions

One of the assumptions of Crisostomi et al. (2011) was that of local flow conservation, i.e., the number of cars entering a road is equal to the number of cars leaving the road. Clearly this assumption is not realistic, as people may park their vehicles at their destination (e.g., home/workplace) for significant time intervals and resume driving the vehicle again at a later

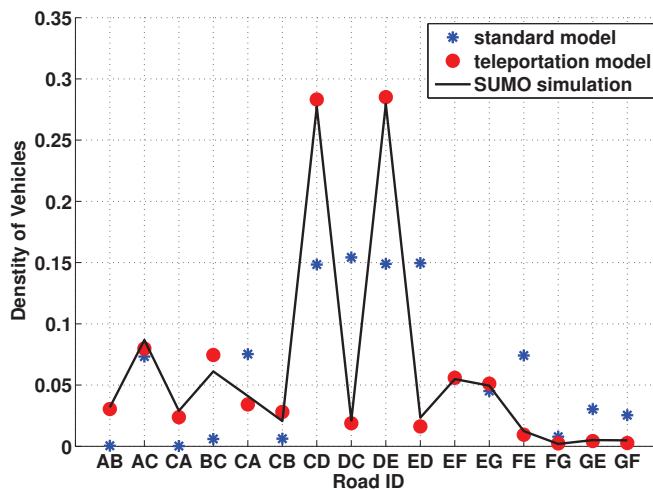


Figure 4. Comparison of simulation results with the models with and without teleportation. The simulated traffic was generated such that the local flow conservation assumption is not valid.

time. Thus, the flow conservation does not hold over reasonable time scales.

We now show that with the extended model, based either on teleportation or the extra state, the flow conservation assumption can be relaxed. For this purpose, we simulate the traffic network depicted in Figure 1 using SUMO by randomly choosing pairs of source/destination roads. To make sure that the local flow conservation assumption is not valid, sources are located mainly in the left triangle, while destination roads can mainly be found in the right triangle. We let cars leave the network as soon as they reach their destination; similarly new cars appear in the network starting from the source road at random times. Figure 4 shows that the teleportation method (whose stationary vector is, as previously stated, a scalar multiple of the appropriate subvector of the stationary distribution obtained by the extra state method) is perfectly coherent with the measurement of the simulations in SUMO. On the other hand, it can be appreciated from the same figure that the previous method completely fails to describe the stationary distribution, as in the example flows of cars are not conserved.

4.2 Optimal Routing

Even for a combustion driven vehicle it is usually hard to find an optimal route, as there are always trade-offs between travel time, travel distance, cost, pollution, etc. Taking the limited range and special requirements of electric vehicles into account certainly adds yet another dimension to this problem. However, contemporary navigational software and path finding algorithms are not taking this new dimension into account and are thus of limited use for the coming generation of vehicles. Our Markov chain model has proven a reliable first step to modelling electric vehicles. In addition, from this model it is possible to derive a number of routing strategies more tailored to the requirements of electric vehicles. We outline some of them in this section. We give details to two of the approaches and plan to work out the other approaches in the near future. These routing strategies may help to promote the cause of electric and hybrid electric vehicles. All of the following routing strategies address distinct issues related to electric vehicles and traffic in general. Each strategy is associated with a different kind of route optimality.

Minimum Energy Routing : A very simple yet important routing strategy for electric vehicles can be obtained by minimising the distance to the destination not in terms of travel

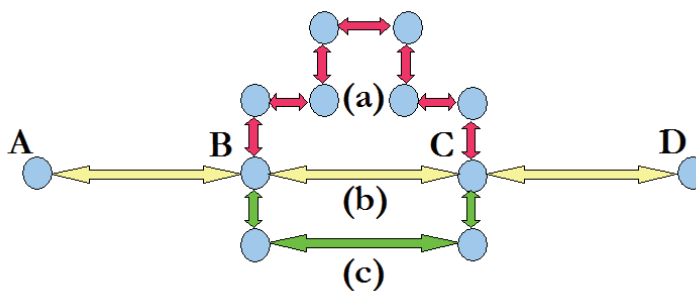


Figure 5. There are three possible paths to go from B to C. Different routing strategies based on minimum distance, minimum energy consumption suggest different paths, also depending on the different environmental conditions (e.g., air conditioning switched on/off).

Table 3. Required energy (in kW) to travel from B to C in the road network depicted in Figure 5

Auxiliary Power Demand	500 W	3500 W
Route (a)	535	924
Route (b)	915	1050
Route (c)	695	884

time or actual distance, but instead in terms of energy charge needed to finish the journey. Using the weights calculated in Section 3.1 combined with a classic graph search algorithm like Dijkstra (1959) it is possible to find minimum energy paths for each origin-destination pair.

Let us consider the road network depicted in Figure 5 as a case study for minimum energy routing. There are three routes connecting B to C. Assume that route (a) is 1.8 km long and is travelled at an average speed of 50 km/h, route (b) is 1 km long and travelled at 80 km/h and route (c) is 1.4 km long and travelled at 80 km/h. Further assume that route (b) is not flat, but rises to a small hill at its center at a constant slope of 5 % in both directions. Table 3 reports the energy required to travel each route calculated with two different powers needed by auxiliary systems in the vehicle. According to Farrington and Rugh (2000) the power demand of accessory systems in an electric vehicle is largely affected by the usage. For instance, the power may vary from a minimum of 500 W to a maximum of 3500 W, for instance in winter, when the heating is running at full power.

Now in travelling from A to D, the driver has a choice to take one of the three routes (a),(b) or (c). The shortest route between B and C is route (b) but we can see in Table 3 that both the longer routes perform better in minimising the required energy for travelling. This is due to the non-flatness of route (b) and the high energy costs for electric vehicles on upward slopes. Additionally, we can see that route (a) is more energy efficient then route (c) if the auxiliary power demand is low, while this relationship is reversed if the auxiliary power demand is high. This implies that, especially in more complex routing tasks, an estimate of the power demand and its changes over time is necessary to achieve efficient and close to optimal solutions.

We believe that it is possible to assist users in making energy conscious route choices by providing energy road maps, i.e. road maps in which the displayed distance corresponds to energy consumption instead of travel distance.

Minimum Popularity Routing : In order to minimise the risk of traffic accidents and congestion along the vehicles path, in some situations it may be advisable to avoid the roads that most people use. Such popular roads could for example be close to shopping areas or train stations. The base Markov chain presented in Section 2.2 describes how often roads are taken, while ignoring travel times or energy consumption. Thus, it carries information about

1 popularity and its stationary distribution can be used to find the minimum popularity route,
2 again using conventional graph search algorithms.
3

4 **Mixed Minimum Energy/Popularity Routing** : Both minimum energy and minimum
5 popularity routing may be too focused on one aspect of traveling. To circumvent this it is
6 possible to use a weighted sum of the above two weights to find an optimal path. In this sum
7 we have an additional tuning parameter that can be set according to how important energy
8 and popularity are considered to be. Similarly it is possible to use the derived electric Markov
9 chain presented in Section 3.2, which contains information about both energy consumption and
10 popularity and use its stationary distribution as weights for the graph search.
11
12

13 **Energy Optimal Risk-Averse Routing** : The limited range of electric vehicles can be
14 managed by choosing appropriate routes, as discussed above, or switching to other modes
15 of transportation for long distances. However, this might only mitigate but not completely
16 eliminate “range anxiety” (i.e., the continual concern and fear of becoming stranded with a
17 discharged battery in a limited range vehicle, Tate et al. (2008)). For instance, unexpected
18 events might require a longer path than expected, and the depletion of the battery before
19 arrival. To avoid this, we propose the following scheme. For each road segment we calculate the
20 impact on the network performance in the case that it is closed (as measured by the Kemeny
21 constant) and use this as a weight for the graph search in order to obtain a route along which
22 incidents have the least impact. This way of routing was first proposed in Crisostomi et al.
23 (2011) in the context of conventional combustion driven vehicles, but its impact on electric
24 vehicle routing is much more significant.
25
26

27 **Socially-Aware Optimal Routing** : All conventional routing algorithms and also the ones
28 described above have a main characteristic in common: they are greedy. That is, they try to
29 achieve the best result for an individual in a given situation. It is well known that this can
30 lead to a suboptimal behaviour of the whole system and as exemplified by Braess (1968) and
31 Braess et al. (2005), this can even cause sub-optimal performance for each individual driver.
32 This problem can be solved by centralised routing, that is a central server computes routes for
33 each vehicle and communicates them to the drivers. This approach is of course associated with
34 a number of problems including the required infrastructure and cooperation of all drivers.
35 We believe that the ideal approach lies in randomised routing, where drivers with coinciding
36 origins and destinations may take different routes. One way of achieving this is to affect the
37 drivers route choices by giving incentives, such as different travel speeds or tax advantages. Our
38 Markov chain framework is very close to this way of thinking and can thus play an important
39 role in this routing strategy. We further claim that in our proposed setup the Kemeny constant
40 can be utilised to measure the global efficiency of a given road network configuration and can
41 thus be used to rate different routing strategies.
42
43
44

45 **Energy Optimal Minimum-Error Routing** : Not only external events such as accidents
46 can cause unplanned route changes. This can also happen by human error. We propose that
47 routes can be chosen in order to minimise the impact that a driving mistake can have on energy
48 demand. We now explore this routing strategies in more detail.
49
50

51 The Markov chain can be used to evaluate possible routes for drivers that are not confident
52 or unfamiliar with the road network and are thus prone to make errors, for example they might
53 take a wrong turn. The following application of the Markovian framework was first proposed in
54 Crisostomi et al. (2011a) and more details can be found there. However, the ideas in Crisostomi
55 et al. (2011a) assume an even greater importance when applied to electric vehicles because of
56 their limited range. In such vehicles the cost of a wrong turn may be high (especially if it leads
57 to a one-way system) as significant battery power may be consumed in correcting the mistake.
58
59
60

Table 4. Expected required energy (in 100 kW) to travel from OA to TO in the network in Figure 6; probability in percent

Error Probability	1	2	3	4	5	6	7	8	9	10
Route 1	1.956	2.036	2.115	2.194	2.273	2.351	2.429	2.506	2.582	2.659
Route 2	2.076	2.117	2.157	2.197	2.237	2.277	2.317	2.357	2.397	2.437

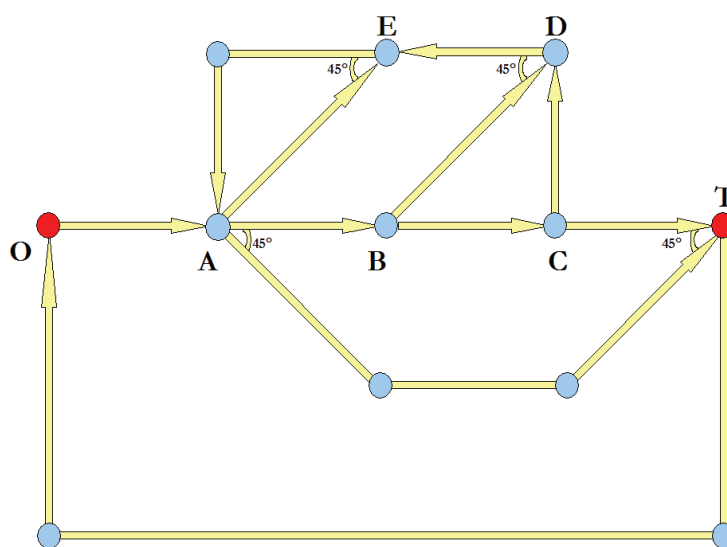


Figure 6. Example of a road network with two possible routes. The route performance depends on the individual driver.

The basic idea, therefore, is to find routing strategies where the cost of making a wrong turn is low.

To see how this may be achieved, consider the road network depicted in Figure 6. There are two reasonable routes a vehicle might take from O to T, Route 1: OA-AB-BC-CT and Route 2: OA-AT. Assume the driver has a probability of making a wrong turn at each junction of $\epsilon > 0$. The routes are evaluated by constructing an individual transition matrix Q for each route, where the probability of making the right turn at each junction is set to $1 - \epsilon$ and all other choices are given the same probability. As a performance indicator we use the MFPE between origin and destination.

In Table 4 we show the MFPE from road segment OA to road segment TO of both routes as a function of the error probability. We can clearly see that Route 1 performs better when the probability of making an error is less than 4%, otherwise Route 2 is superior. For this example we used a constant cruising speed of 50 km/h on each road segment and travel times proportional to the length of each road.

As can be observed, the robust routing algorithm is particularly appealing in the case of electric vehicles, as a driving mistake might lead to a longer path and an unexpected higher energy consumption. The situation gets even worse if the driver ends up in a zone without charging stations.

Comment : Note that routing for electric vehicles is particularly challenging. This follows from the fact that energy is scarce in electric vehicles, and that significant amounts of energy can be consumed by on-board systems. This means that the time taken for a journey is important if the energy consumption per unit time is high. For example, in winter when the vehicle is being heated, or in summer when the air-conditioner is used, the duration of the journey becomes

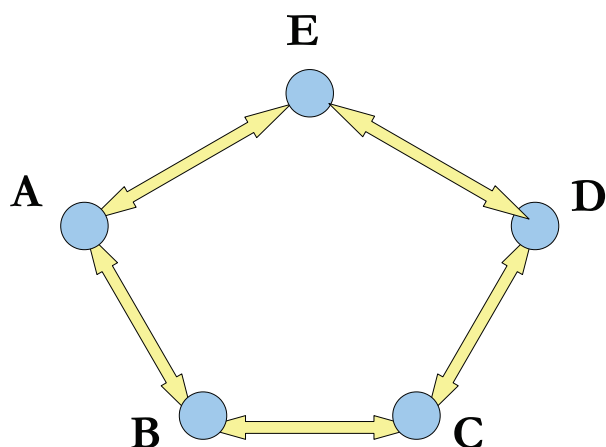


Figure 7. An example road network.

very important. In contrast, when the energy consumption is low, optimal routes depend mostly on road network topology and cruising speed. One fundamental observation about travelling is: The slower the cruising speed is, the less energy is consumed per unit of distance. Thus, given a choice between a low speed route and a high speed route of similar length, it is apparently better to take the low speed route. However, given the time dependence discussed above, this is not entirely true.

To illustrate this basic point, consider the traffic network depicted in Figure 7. We determine the stationary distribution of energy dissipation for two scenarios, corresponding to the air-conditioner being switched on and off. To achieve this, we assume a constant base load of 500 W in the first scenario and a load of 3500 W in the second scenario (Farrington and Rugh 2000). There are two routes to travel from A to D: the northern route (AE-ED) and the southern route (AB-BC-CD). Let speed limits of 50 km/h on the northern route and 30 km/h on the southern route be given. In this situation one notices two facts:

- In travelling from A to D the minimum energy route with air-conditioner on is the northern route, while with air-conditioner off it is the southern route. This means that optimal route calculation is dependent on driver preferences. Issues like the weather have to be taken into account.
- The stationary distributions corresponding to the two scenarios are given in Figure 8. Note that the stationary properties of the network are very different in the two cases.

4.3 Traffic Load Control

Being able to control the stationary distribution of a road traffic network opens up a wide range of possibilities and different applications. For many goals corresponding optimal stationary distributions can be calculated and the system can then be driven towards them. For example, using the congestion chain it may be possible to equalise the travelling time on parallel routes to distribute the load within the network. Alternatively road network designers may be able to unburden some road segments in order to facilitate maintenance activities. In the context of the pollution chain, it may be interesting to be able to dissolve pollution peaks or even to minimise pollution along some roads or sub-networks in critical areas, for example near hospitals or schools. As we are primarily interested in the modelling of electric vehicles in this present work, we regard the Perron vector control in this context. While it is not as apparent what the advantage is of reducing energy consumption along an individual road for example, there

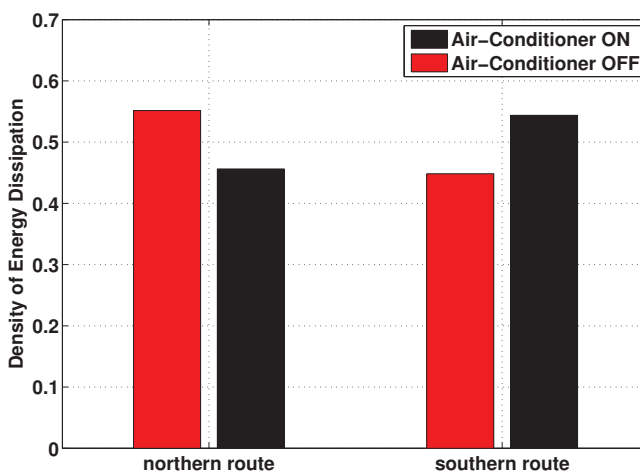


Figure 8. Stationary distribution of energy dissipation in two cases.

Table 5. Speed limits (in km/h) in the uncontrolled case, in the unrealistic optimal solution, and in the realistic balanced case

Road Segment	AB	AC	BA	BC	CA	CB	CD	DC
Uncontrolled Case	50	50	50	50	50	50	50	50
Optimal (Unrealistic) Case	15	44	15	29	44	29	117	122
Realistic Solution	30	50	30	40	50	40	100	100

Road Segment	DE	ED	EF	EG	FE	FG	GE	GF
Uncontrolled Case	50	50	50	50	50	50	50	50
Optimal (Unrealistic) Case	117	117	45	21	42	10	23	8
Realistic Solution	100	100	50	40	50	30	40	30

are many applications which benefit from the ability to control the stationary distribution. From a network designing point of view it may be interesting to be able to match high energy consumption with free charging point capacity. This can be used to equalise the demand on each charging stations. Furthermore a basic concern of road network planners is to make the best use of available resources. The efficiency (or total energy cost) of a network can be measured by the Kemeny constant. The Kemeny constant in turn can be viewed as a function that is dependent on stationary distribution. It may thus be possible to influence the Kemeny constant by controlling the stationary distribution and we plan to investigate the control of the Kemeny constant in the near future. We now investigate in more detail how the Perron vector of our chain can be controlled.

4.3.1 Theoretical Approach

Lemma 1 suggests a simple strategy to regulate the Perron eigenvector of the chain. Note that the Perron vector is determined by the Perron vector of the basic chain, and the diagonal scaling. The scaling in turn is determined by a host of factors, some of which can be controlled by the network designer. One of these is the speed limit (already some cities in Austria have adaptive speed limits). Recall that if the left Perron vector of \mathbb{P} is x^\top and we wish through feedback to achieve a target left eigenvector z^\top of \mathbb{Q} for some positive vector $z = (z_1, \dots, z_n)^\top$ we set $w_i = \frac{z_i}{x_i}$ according to Lemma 2.1.

A useful application of the Perron vector control is now illustrated through an example which exploits again the road network of Figure 2. The dashed line in Figure 9 depicts the nominal density of cars in the case of uniform speed limits set to 50 km/h. Let us assume that the road engineer is interested in manipulating speed limits in order to achieve a uniform density of cars along all road segments (traffic balancing). Lemma 1 can be used to compute the “optimal”

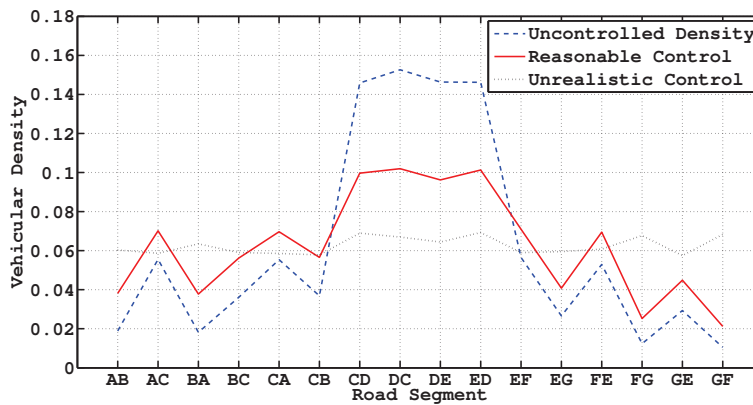


Figure 9. Comparison of traffic density as a function of speed limits. Uniform speed limits lead to the unbalanced solution shown with a dashed line. A very good balance, in dotted line, is achieved using the unrealistic speed limits reported in Table 5, second line. A trade-off solution shown with solid line is obtained by using realistic speed limits as shown in Table 5, third line.

weights, and predict the “optimal” speed limits accordingly. New simulations in SUMO show that the desired objective is indeed obtained, as shown with a dotted line in Figure 9, although such “optimal” speed limits are unrealistic, as shown in Table 5, second line. A good trade-off is shown with solid line in Figure 9, where reasonable speed limits are used instead (e.g., they are all multiples of 10), as reported in the third line of Table 5.

Comment : The proposed application assumes that drivers will not change their routes as a reaction to the new imposed speed limits; we also varied speed limits under the implicit assumption that this would correspond to proportionally adjust average travel speeds. Despite these assumptions, Figure 9 shows that the road network traffic, as observed from SUMO simulations, is in accordance with the theory.

4.3.2 Decentralised Traffic Load Control

In the section above we controlled the Perron vector by choosing appropriate weights in the graph. This weight is however not necessarily something we can access directly. In a realistic scenario we may be able to change speed limits or traffic light sequencing to affect the weight, but the relation to the weight is not explicitly given. We use an algorithm from Stanojević and Shorten (2009), which presents a decentralised way to reach an implicit consensus. We present two simulations using this algorithm. In the first example we take a large road network and one junction with three incoming streets and one outgoing street, as depicted in Figure 10. We adjust the speed limits on the three incoming streets such that the amount of energy required to traverse these streets is equalised. In the second example the large road network is regarded as consisting of two main components that are connected by 4 bridging streets as depicted in Figure 11. In order for the algorithm to function, each road segment is assumed to be able to measure the density of cars travelling on the road, and to communicate this information to neighbouring roads.

As proposed in a different context in Stanojević and Shorten (2009), our objective here is to determine speed limits that equalise the load across certain road segments. To this end let \mathcal{I} be the set of road segments of interest, let us discretise time in steps $k = 1, 2, \dots$ and let speed limits $v_i(0)$ at time $k = 0$ be given for all $i \in \mathcal{I}$. Let us denote by $\theta_i(k)$ the density of energy dissipated on each road segment for all $k = 1, 2, \dots$. Then we use the following iterative equation to update the speed limits

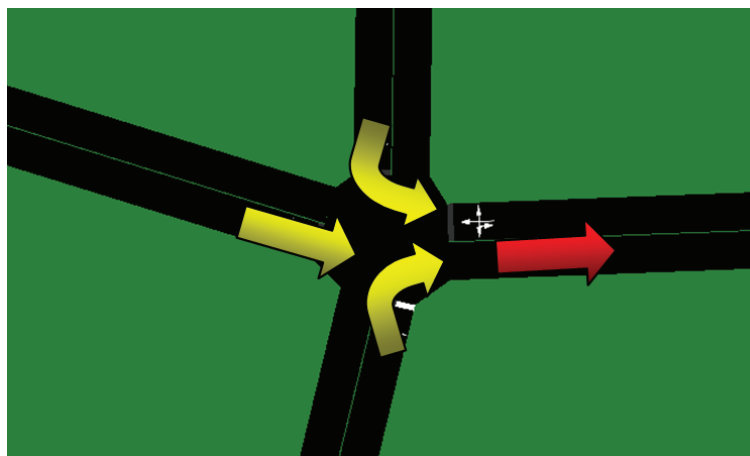


Figure 10. Scenario with three streets with a common continuation, where we try to equalise the amount of energy expended on each street.

$$v_i(k+1) = v_i(k) + \eta \sum_j (\theta_j(k) - \theta_i(k)), \tag{33}$$

where η is a positive parameter and the sum is taken over all road segments $j = 1, \dots, n$ that road i can communicate with.

The implicit consensus is conducted by alternating the following two steps:

- (1) Determine densities of interest (e.g., energy dissipation) at time k .
- (2) Update speed limits according to Equation (33).

For our two examples we used SUMO simulation runs and calculated the stationary distribution of the energy Markov chain. As the density of each road segment we used the corresponding entries of the stationary distribution. We performed an update of the speed limits according to Equation (33) and continued with the next instance of the simulation. In Figures 12 and 13 we give the relevant entries of the stationary distribution as a function of the number of simulation runs. Full details of the algorithm are given in Stanojević and Shorten (2009). At this point we just use the implicit consensus algorithm without proving that it achieves the balancing of the stationary vector. We intend to do this in our future work.

5 Conclusions

In this paper we have reviewed an approach to modelling road network dynamics using Markov chains. We improved the original framework proposed in (Crisostomi et al. 2011) by mathematically proving consistency of the model and the relevant notions of interest, and by relaxing the flow conservation assumption to allow realistic road network scenarios. The model was generalised to describe the battery consumption for electric vehicles in the road network, and as the battery level can locally increase due to regenerative braking effects, this required a suitable modification of conventional Markov chain theory to handle energy distributions with possible negative values. Possible applications of the proposed theory, such as optimal routing and traffic load control, have been illustrated and validated through the support of the mobility simulator SUMO.

One of the main impediments to a capillary adoption of the electric vehicle technology is



Figure 11. Scenario of a big city and a suburb with 4 connecting streets, where we try to equalise the amount of energy expended on each street out of the suburb.

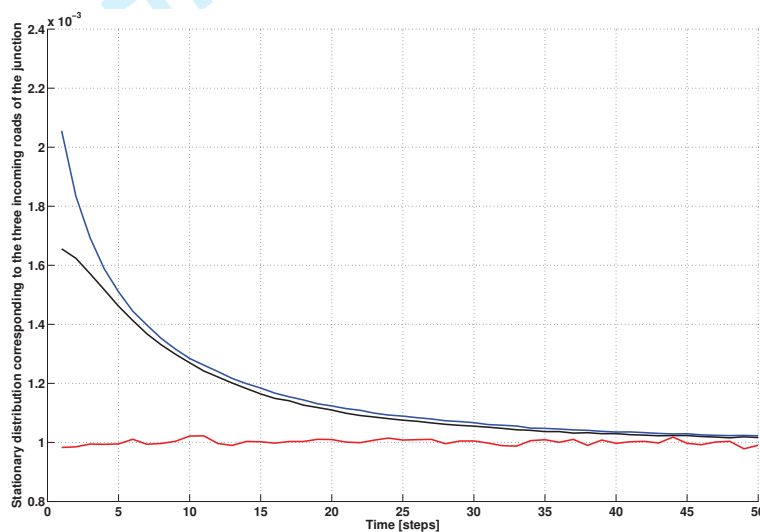


Figure 12. Convergence results for the single junction scenario. The vertical axis shows the corresponding entries of the Perron vector. Each time step corresponds to one simulation instance.

believed to lie in the users' perception that the range of the vehicles is limited and there is a non-negligible risk of remaining stranded with a discharged battery (also known as "range anxiety"). The final objective of this work is to provide a theoretical framework that can be used as a basis for deriving applications (e.g., minimum energy routing) that can mitigate such a fear and ultimately encourage a behavioural change towards the electric vehicle technology. In this view, future work will be concerned in both experimentally validating the proposed theory and algorithms, and in developing further applications, based on the same framework, that can support an optimal exploitation of electric vehicle and sustainable management of traffic in general.

Acknowledgements

The authors would like to thank the (anonymous) reviewers whose remarks contributed to improve the quality and the clarity of the final version of this article. They also thank Audrey La Louze and Faustine Richaud both from Université de Provence in Marseille for helpful discussions

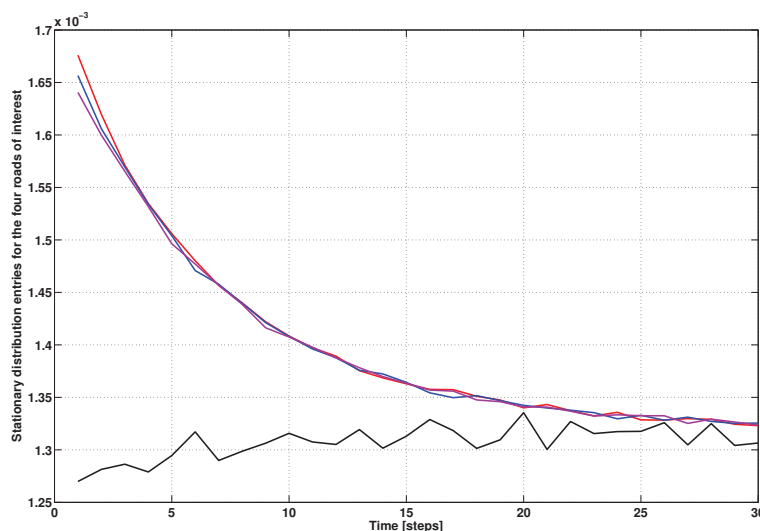


Figure 13. Convergence results for the suburb scenario. The vertical axis shows the corresponding entries of the Perron vector. Each time step corresponds to one simulation instance.

that helped writing the section about alternative flow conservation assumptions. Stephen Kirkland is supported in part by the Science Foundation Ireland under Grant No. SFI/07/SK/I1216b. Robert Shorten and Emanuele Crisostomi are supported in part by Science Foundation Ireland under grant number PI Award 07/IN.1/1901. Arie Schlote is supported in part by HEA grant PRTL15 TGI.

References

- Baskar, L., De Schutter, B., Hellendoorn, J., and Papp, Z., *Traffic control and intelligent vehicle highway systems: a review*, Vol. 5, IET Intelligent Transport System (2011).
- Berman, A., and Plemmons, R., *Nonnegative Matrices in the Mathematical Sciences*, SIAM (1994).
- Biem, A., Bouillet, E., Feng, H., Ranganathan, A., Riabov, A., Verscheure, O., Koutsopoulos, H., Rahmani, M., and Güç, B. (2010), “Real-Time Traffic Information Management using Stream Computing,” *IEEE Data Engineering Bulletin*, 33.
- Braess, D. (1968), “Über ein Paradoxon aus der Verkehrsplanung,” *Unternehmensforschung*, 12, 258 – 268.
- Braess, D., Nagurney, A., and Wakolbinger, T. (2005), “On a Paradox of Traffic Planning (translation from the German original),” *Transportation Science*, 39, 446 – 450.
- Chen, H., and Yao, D., *Fundamentals of queueing networks: performance, asymptotics, and optimization*, Vol. 46 of *Applications of mathematics :stochastic modelling and applied probability*, Springer (2001).
- Crisostomi, E., Kirkland, S., Schlote, A., Shorten, R., and (Kim, J. and Lee, M., Eds.), (2011b) *Markov Chain based Emissions Models: a Precursor for Green Control (Green IT: Technologies and Applications, pp. 381-400)*, Springer Verlag.
- Crisostomi, E., Kirkland, S., and Shorten, R. (2011), “A Google-like model of road network dynamics and its application to regulation and control,” *International Journal of Control*, 84, 633–651.
- Crisostomi, E., Kirkland, S., and Shorten, R. (Milan, Italy, 2011a), “Robust and risk-averse routing algorithms in road networks,” in *IFAC World Congress*.
- Dellnitz, M., and Junge, O. (1999), “On the approximation of complicated dynamical behaviour,” *SIAM J. Numer. Anal.*, 36, 491–515.
- Dellnitz, M., Junge, O., Koon, W., Lekien, F., Lo, M., and Marsden, J. (2005), “Transport

- 1 in dynamical astronomy and multibody problems,” *International Journal of Bifurcation and*
 2 *Chaos in Applied Sciences and Engineering*, 3, 699–727.
- 3 Dijkstra, E. (1959), “A note on two problems in connexion with graphs,” *Numer. Math.*, 1, 269
 4 – 271.
- 5 Dirks, S., Gurdgiev, C., and Keeling, M., *Smarter cities for smarter growth, How cities can*
 6 *optimize their systems for the talent-based economy*, IBM Global Business Services Executive
 7 Report (2010).
- 8 Farrington, R., and Rugh, J. (2000), “Impact of Vehicle Air-Conditioning on Fuel Economy,
 9 Tailpipe Emissions, and Electric Vehicle Range; Preprint,” in *Earth Technologies Forum,*
 10 *Washington, D.C.*
- 11 Froyland, G., *Extracting dynamical behavior via Markov models*, Nonlinear dynamics and statis-
 12 tics (Cambridge, 1998), Birkhäuser Boston, Boston (2001).
- 13 Grinstead, C., and Snell, J., *Introduction to Probability*, 2nd edition ed., American Mathematical
 14 Society (2003).
- 15 Hartenstein, H., and Laberteaux, K., *VANET / Vehicular Applications and Inter-Networking*
 16 *Technologies*, Wiley (2010).
- 17 Horn, R., and Johnson, C., *Matrix Analysis*, Cambridge University Press (1990).
- 18 Huisinga, W. (2001), “Metastability of Markovian Systems: A Transfer Operator Based Ap-
 19 proach in Application to Molecular Dynamics,” Freie Universität Berlin.
- 20 Hunter, J. (2006), “Mixing times with applications to perturbed Markov chains,” *Linear Algebra*
 21 *Appl.*, 417, 108–123.
- 22 Kemeny, G., and Snell, J., *Finite Markov Chains*, Van Nostrand (Princeton, 1960).
- 23 Koon, W., Lo, M., Marsden, J., and Ross, S. (2000), “Heteroclinic connections between periodic
 24 orbits and resonance transitions in celestial mechanics,” 10, 427–469.
- 25 Koon, W., Marsden, J., Ross, S., and Lo, M. (2002), “Constructing a low energy transfer
 26 Constructing a low energy transfer between Jovian moons,” in *Contemporary Mathematics*, Vol.
 27 292, pp. 129–145.
- 28 Krajzewicz, D., Bonert, M., and Wagner, P. (Bremen, Germany, 2006), “The open source traffic
 29 simulation package SUMO,” in *RoboCup 2006 Infrastructure Simulation Competition*.
- 30 Langville, A., and Meyer, C., *Google’s Page Rank and beyond—The science of search engine*
 31 *rankings*, Princeton University Press, Princeton (2006).
- 32 MacKay, D., *Sustainable Energy - Without the Hot Air*, Uit Cambridge Ltd. (2008).
- 33 Meyer, C. (1989), “Uncoupling the Perron eigenvector problem,” *Linear Algebra Appl.*, 114,
 34 69–94.
- 35 Moya, S., and Poznyak, A., *Extraproximal Method Application for a Stackelberg-Nash Equilibrium*
 36 *Calculation in Static Hierarchical Games*, Vol. 39, IEEE Transactions on Systems, Man, and
 37 Cybernetics - Part B: Cybernetics (2009).
- 38 Piccoli, B., and Garavello, M., *Traffic Flow on Networks*, American Institute of Mathematical
 39 Sciences (2006).
- 40 Qian, K., Zhou, C., Allan, M., and Yuan, Y. (2011), “Modeling of Load Demand Due to EV
 41 Battery Charging in Distribution Systems,” *IEEE Transactions on Power Systems*, 26.
- 42 Schütte, C., and Huisinga, W., *Biomolecular conformations can be identified as metastable sets*
 43 *of molecular dynamics*, Vol. x of *Handbook of Numerical Analysis*, North-Holland, Amsterdam
 44 (2003).
- 45 Stanojević, R., and Shorten, R. (2009), “Generalized distributed rate limiting,” in *In IWQoS’09:*
 46 *Proceedings of 17th IEEE International Workshop on Quality of Service*, July, Charlston, SC,
 47 USA, pp. 1–9.
- 48 Tate, E., Harpster, M., and Savagian, P. (2008), “The Electrification of the Automobile: From
 49 Conventional Hybrid, to Plug-in Hybrids, to Extended-Range Electric Vehicles,” in *SAE World*
 50 *Congress & Exhibition, Detroit. Reprinted from: Advanced Hybrid Vehicle Powertrain*.
- 51 Villa, N., and Mitchell, S. (2009), “Connecting cities: achieving sustainability through innova-
 52 tion,” in *Fifth Urban Research Symposium 2009: Cities and Climate Change: Responding to*
 53
 54
 55
 56
 57
 58
 59
 60

1 *an Urgent Agenda, Marseille, France.*
2
3
4
5
6
7
8
9
10
11
12
13
14
15
16
17
18
19
20
21
22
23
24
25
26
27
28
29
30
31
32
33
34
35
36
37
38
39
40
41
42
43
44
45
46
47
48
49
50
51
52
53
54
55
56
57
58
59
60

For Peer Review